Case Studies in Thermal Engineering 27 (2021) 101238

Contents lists available at ScienceDirect

Case Studies in Thermal Engineering

journal homepage: www.elsevier.com/locate/csite

Experimental investigation of the microbubble generation using a venturi-type bubble generator

Kittipong Sakamatapan [a], Mehrdad Mesgarpour [a], Omid Mahian [b,c], Ho Seon Ahn [d,**], Somchai Wongwises [a,e,*]

[a] Fluid Mechanics, Thermal Engineering and Multiphase Flow Research Lab (FUTURE), Department of Mechanical Engineering, Faculty of Engineering, King Mongkut's University of Technology Thonburi (KMUTT), Bangkok, 10140, Thailand
[b] School of Chemical Engineering and Technology, Xi'an Jiaotong University, Xi'an, China
[c] Department of Mechanical Engineering, Center for Nanotechnology in Renewable Energies, Ferdowsi University of Mashhad, Mashhad, Iran
[d] Department of Mechanical Engineering, Incheon National University, Republic of Korea
[e] National Science and Technology Development Agency (NSTDA), Pathum Thani, 12120, Thailand

ARTICLE INFO

Keywords:
Microbubble
Microbubble generator
Venturi
Entry angle
Exit angle

ABSTRACT

This experimental study investigated how changes in the water flow rate affected the number and size of microbubbles using venturi with equal entry and exit angles of 30°. The water flow rate ranged between 10 and 18 m^3/h . Photos of microbubbles were taken with a digital camera in a visualized section that was specifically installed to store a certain amount of water to measure microbubble size and the number of microbubbles. The experimental results indicated that when the water flow rate increased, the airflow rate also increased. The microbubble size tended to decrease when the water flow rate increased; the sizes obtained were in the range of 50–130μm. The amount of air bubbles tended to increase when the water flow rate increased.

1. Introduction

Microbubbles can be used diversely in daily life, for example, for treatment of wastewater at the community or larger-than-community level, addition of oxygen in wastewater and so on.

A microbubble is a tiny air bubble with a diameter of 5–200 μm. Microbubbles have a large contact surface that helps in trapping dirt. Compared with bubbles that have a larger-than-micrometer-level diameter, microbubbles have a lower buoyant force that slows down their buoyant speed. Lee et al. [1] studied the size of microbubbles created from a venturi nozzle with various entry and exit angles. They adjusted both angles in five steps – 15, 22, 30, 38, and 45° – to find the bubble size at each angle. The water flow rate used ranged from 140 to 300 LPM to study airflow rate, pressure drop, and bubble size. Their findings revealed that entry and exit angles were significant variables. The entry angle had no effect on bubble size but directly affected air suction into the venturi. On the other hand, the exit angle was a major factor in changes of bubble size. They found that the bubble's diameter decreased when the exit angle increased to more than 30°. When the water flow rate was in the range of 260–300 LPM, the bubble's diameter would decrease when the exit angle was over 30°. Hence, they concluded that 30° was the best exit angle for the venturi in terms of pressure drop and airflow rate. The exit angle of 30° could also be used in experiments to determine bubble size. Later, Li et al. [2] extended the previous

* Corresponding author. King Mongkut's University of Technology Thonburi (KMUTT), Bangkok, 10140, Thailand.
** Corresponding author.
E-mail addresses: hsahn@inu.ac.kr (H.S. Ahn), somchai.won@kmutt.ac.th (S. Wongwises).

https://doi.org/10.1016/j.csite.2021.101238
Received 18 April 2021; Received in revised form 7 July 2021; Accepted 9 July 2021
Available online 10 July 2021

experiment by studying how new variables affected the microbubble size.Their experimental variables focused on the physical shape of a venturi-type bubble generator. In their first experiment, they adjusted the diameter of the inlet air hole to 1, 1.5, 2, 2.5, and 3 mm. In the second experiment, they adjusted the number of inlet air holes to 1, 2, and 4 holes. In the last experiment, they adjusted the venturi outlet angle to 7.5, 10, and 12.5°. The control variables were airflow rate in the range of 0.005–0.1 m^3/h and water flow rate in the range of 5–20 m^3/h. They concluded from their experimental results that the diameter and number of inlet air holes had no influence on the microbubble size. On the contrary, the microbubble size would inversely vary with the venturi exit angle. Gordiychuk et al. [3] also studied variables that affect the size of microbubbles by simulating a venturi-type microbubble generator with independent variables of a water flow rate between 13 and 30 LPM, air flow rate between 0.0003 and 0.002 LPM, and air inlet diameter of 0.2–1.5 mm, and then capturing images. Their results indicated that the microbubble size inversely varied with the water flow rate but directly varied with the airflow rate, whereas the air inlet size had no effect. Yin et al. [4] conducted an experiment with venturi-type bubble generation to evaluate the distribution of bubble size in turbulent flow. The relationship between bubble size, surface tension coefficient, and Reynolds number were investigated. Wang et al. [5] conducted an experiment with a novel swirl-venturi microbubble generator. Three different breakup characteristics could be detected.

Fujiwara et al. [6] proposed a technique for producing microbubbles using a converging-diverging nozzle. Their objective was to explain the effects of flow velocity at the throat on the bubble behaviour. Vilaida et al. [7] focused on the settings of an apparatus to find a suitable air-to-water ratio for the best microbubble generation for various sizes of venturi: 3, 4, and 5 mm. Microbubbles were also used to treat wastewater in a community. They found that the venturi with a throat diameter of 3 mm could generate more microbubbles than tubes of other sizes could. Afisna et al. [8] studied a porous-venturi microbubble generator with a 30-degree inlet angle and 20-degree outlet angle. Bubble distribution was measured using a Phantom Control camera. Data were analyzed with MATLAB, whereas the efficiency of the microbubble generator was determined. Liew et al. [9] evaluated the efficiency of aeration using a porous venturi-orifice bubble generator. Increasing water flow through the venturi and orifice ring reduced pressure and later increased cavitation.

Swart et al. [10] studied microbubble behavior generated by a turbine pump. The study was done with a microbubble size of *50-150 μm.* It was concluded that when the outlet pressure of the pump decreased from *0.4* to *0.*2 MPa, the average microbubble size would increase from *86* to *129 μm.*

Suwartha et al. [11] analyzed the effects of size change on the mass transfer coefficient and rising velocity. It was found that the mass transfer coefficient increased with a decreasing microbubble diameter.

Bhadran et al. [12] used a micro-venturi tube to generate controlled monodispersed bubbles in a micro-venturi tube. The venturi tube was 40 *μm* deep. The experimental findings revealed that microbubble size was not limited by the size of the micro-venturi channel. Changes in the bubble size and bubble velocity varied according to the flow parameters.

Previous experiments (Lee et al. [1]) revealed that at a fixed entry angle (α) of 15° and varying exit angles (β) of 15, 22, 30, 38, and 45°, the β of 30° yielded the highest amount of sucked-in air at the same water flow rate, and they found that the α does not directly affect bubble size. Thus, in the present study, the venturi with equal α and β of 30° was chosen for ease of design and to create micron-sized microbubbles. Five water flow rates were used (10, 12, 14, 16, and 18 m^3/h) to determine the number of bubbles and bubble size.

2. Experimental apparatus and procedure

The apparatus is shown in Fig. 1. The operation started when the pump pumped water from the reservoir up to the rotameter with a valve to adjust the flow rate [1,13]. The flow rate of water sent to the venturi was first fixed to a certain level. The flow rate of air

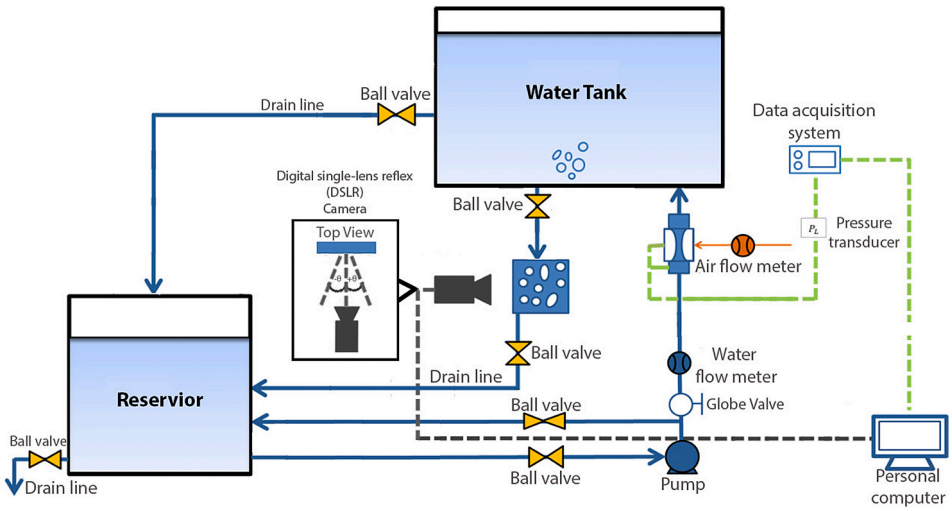

Fig. 1. Schematic of the experimental apparatus.

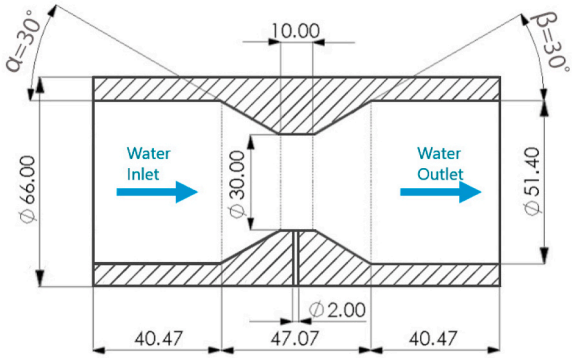

Fig. 2. Schematic of the venturi.

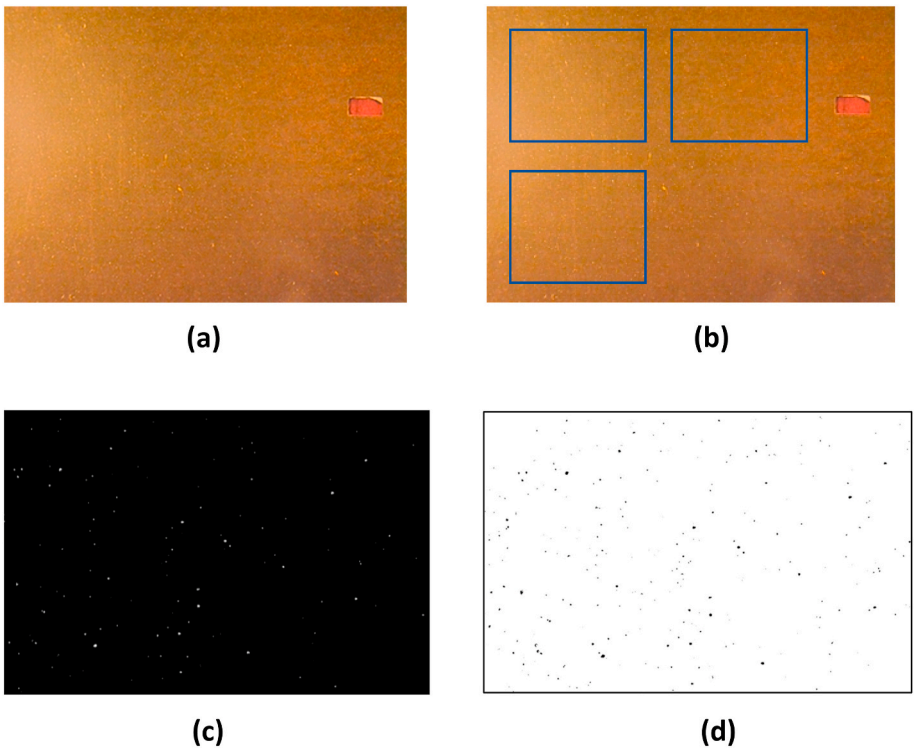

Fig. 3. Postprocessing for determining the sizes of the microbubbles. (a) Raw image (b) Separating the raw image into three parts (c) Converting to 8-bit type (B/W monotone), strengthening the contrast, and erasing the residual pixels, (d) Converting to black and white.

sucked into the venturi was detected by a rotameter (2% full scale accuracy). Next, water with air bubbles formed would move to the water tank and further to the visualized section for photos to be taken and used for later measurement of microbubble size. After that, the remaining water was sent back to the reservoir.

Fig. 2 shows the venturi used in the present study. The entry (α) and exit (β) angles are 30°. When the venturi received water from the pump, water would flow through the venturi's throat, whereas the installed air tube sucked air into it. This is because the inside of the venturi has lower air pressure than the outside. In venturi, when the cross-sectional area was expanded, the pressure would recover and force to break air bubbles into micrometer-sized bubbles**.** The measurement of microbubble size was done using a digital camera to take photos through a clear acrylic box partially containing water. After photographing, photos were fed into an image-processing program (ImageJ) to measure bubble size (see Fig. 3).

First, the photo was divided into three parts, and image scales were set to determine bubble size. Then, the images were converted into 8-bit type to subtract the color and background so that the bubbles would be clearly seen. After subtracting the background, if the

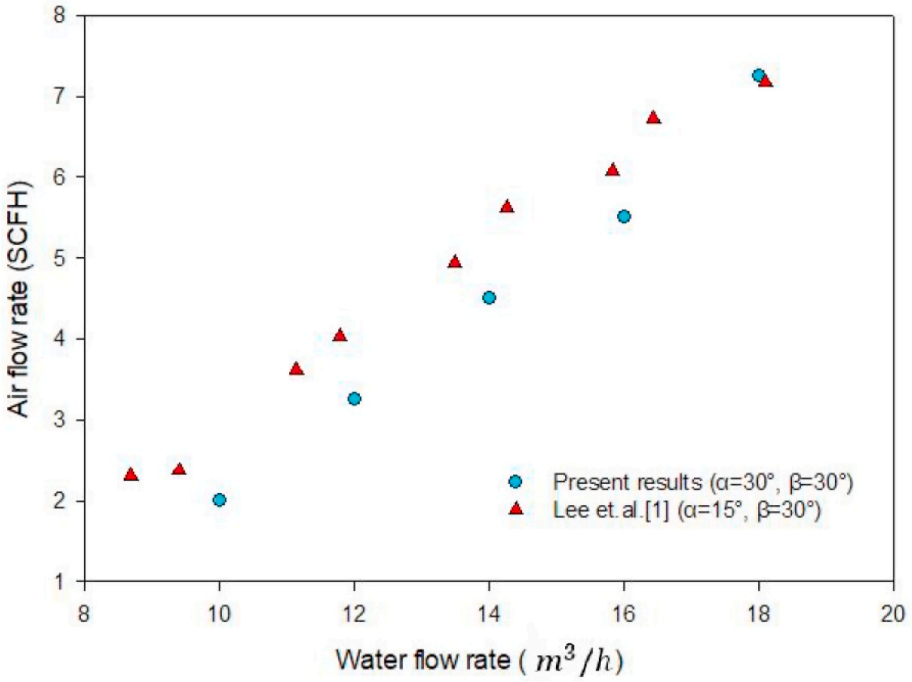

Fig. 4. Air flow rate and water flow rate obtained from the present study and literature.

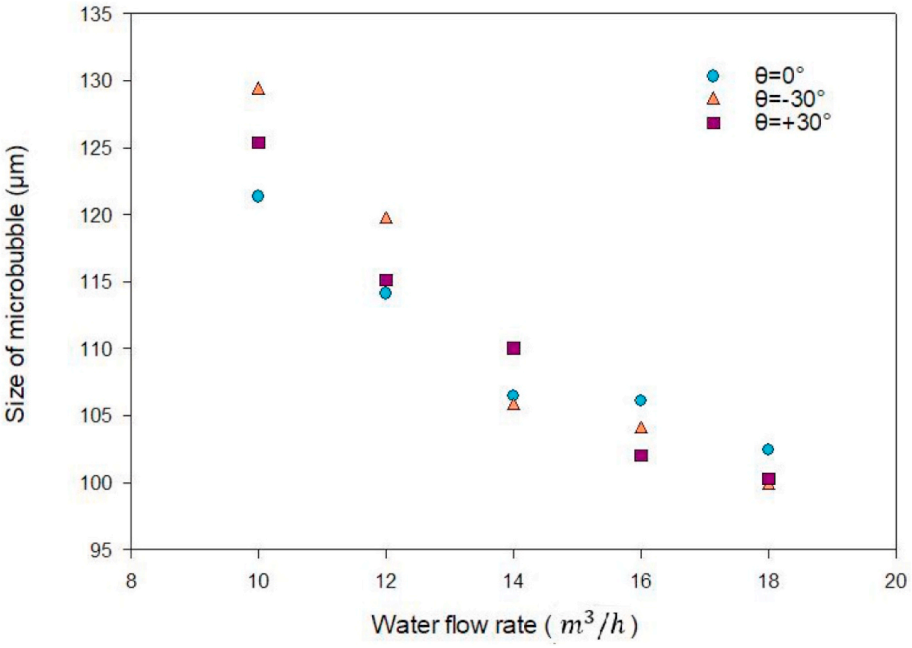

Fig. 5. Size of microbubbles visualized from three locations at various water flow rates.

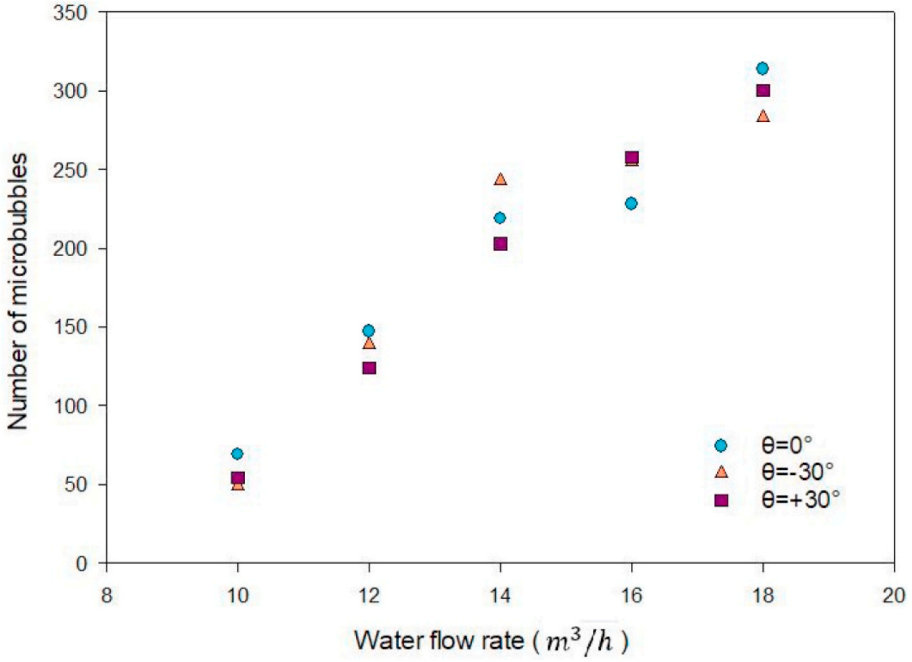

Fig. 6. Number of microbubbles visualized from three locations at various water flow rates.

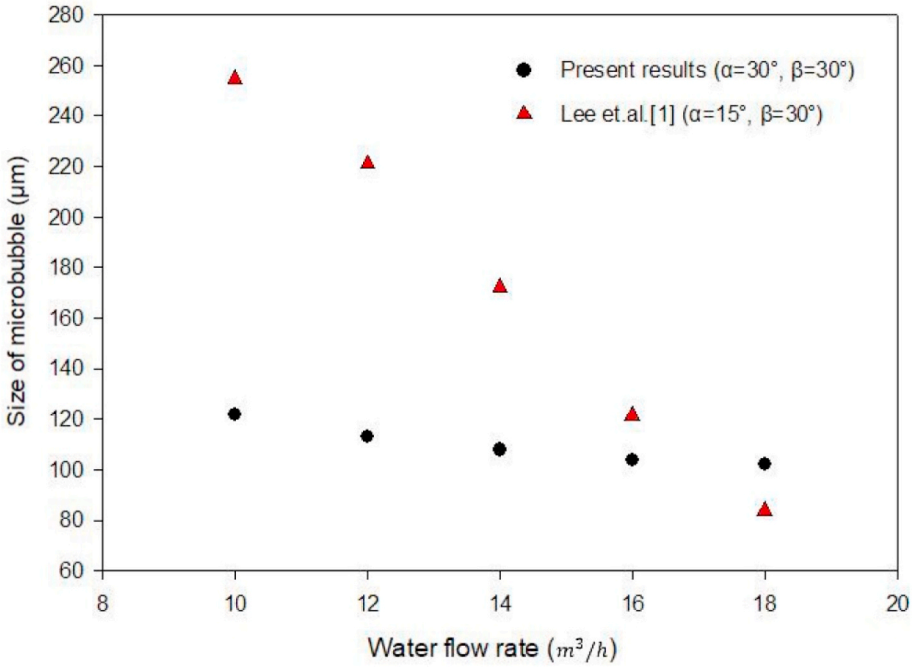

Fig. 7. Relationship between the size of the bubble and water flow rate.

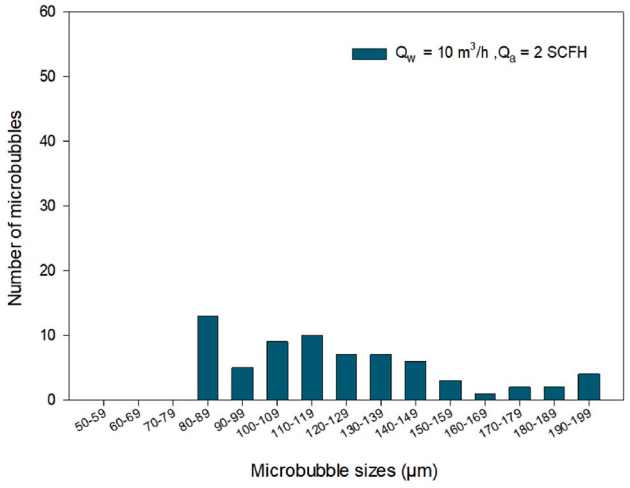

(a)

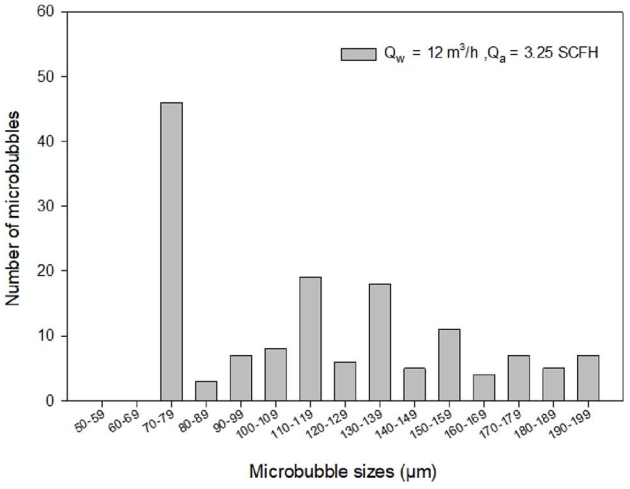

(b)

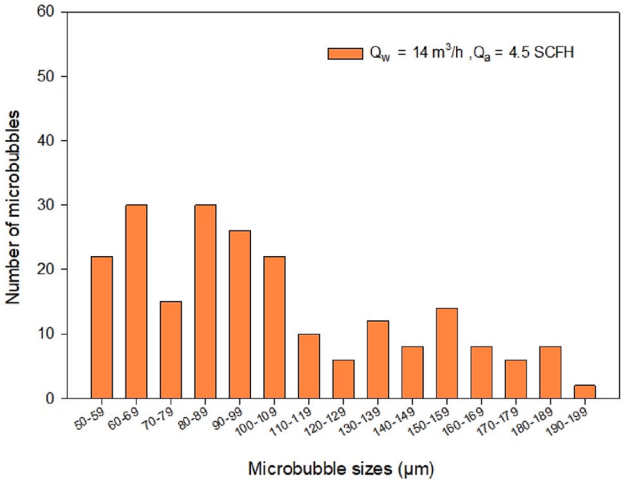

(c)

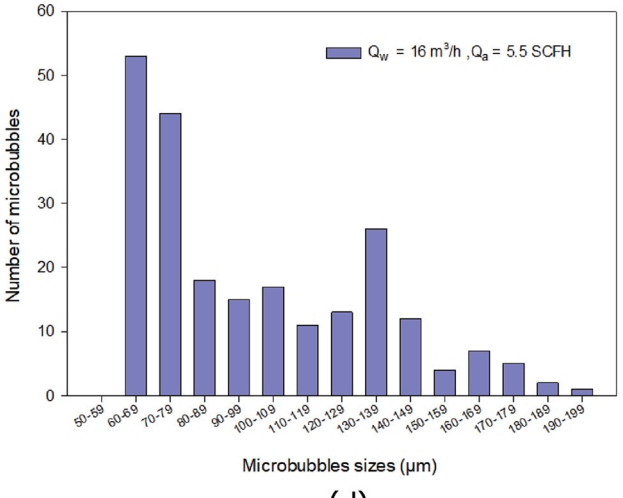

(d)

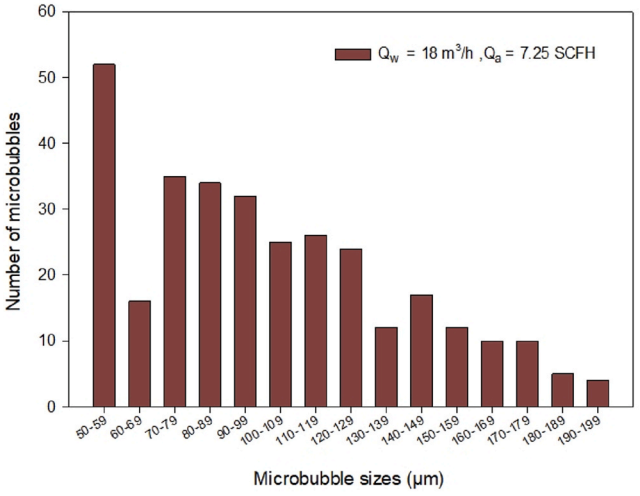

(e)

(caption on next page)

Fig. 8. The number of bubbles at various bubble sizes for water flow rates of (a)10 m^3/h, (b) 12 m^3/h, (c) 14 m^3/h (d) 16 m^3/h and (e) 18.m^3/h

images were still unclear in parts that did not include bubbles, the images' brightness/contrast was adjusted to eliminate the residual pixels. Then, the threshold was adjusted to make the microbubbles clearer and eliminate more residual pixels. Next, all bubble areas could be measured, and results from all three photos would be calculated for average value.

3. Result and discussion

In this experiment, the water flow rate used ranged from 10 m^3/h to 18 m^3/h, with a 2 m^3/h increment at each level. This led to various corresponding air flow rates, as shown in Fig. 4. When compared with the data obtained from the study of Lee et al. [1], who used venturi with a 15-degree entry angle and 30-degree exit angle, it can be seen that the air flow rate obtained from Lee et al. [1] was higher at the same water flow rate. As shown in Fig. 5, when the water flow rate increased, the microbubble size decreased, with the largest bubble size (120–130 μm) at the water flow rate of 10 m^3/h and the smallest bubble size (100 μm) at the water flow rate of 18 m^3/h. When the water flow rate increases, equivalently with an increase in the flow velocity, the inertia effect increases [14]. By overcoming the surface tension effect [15], this dominating inertia effect leads to a decrease in the bubble diameter. Results from photos taken at all three locations also showed the same trend. The amount of microbubbles also increased when the water flow rate increased. The lowest amount of microbubbles was 50–70 at a water flow rate of 10 m^3/h. The highest amount of microbubbles of 270–320 was obtained at 18 m^3/h . The amount of microbubbles measured from photos taken from three different angles showed a similar trend, as seen in Fig. 6. The size of microbubbles in the study of Lee et al. [1] was larger at a water flow rate lower than 18 m^3/h and became smaller at the water flow rate of 18m^3/h, as shown in Fig. 7.

Results from measuring the number of microbubbles that occurred in the water flow rate range of 10–18 m^3/h indicated that, at the lowest water flow rate, there was a small number of small microbubbles, with the smallest size of 80–89 μm. Our observation can be explained as follows: as the water flow rate increases, the flow velocity also increases. The higher flow velocity is suggestive of a relatively stronger inertia effect being acting during the bubble generation phenomenon. In particular, the stronger inertia surpasses the surface tension effect following the viscous shearing effect [16], which is responsible for the bubble generation, and this results in a reduction in the size of the bubble. At the maximum water flow rate, there were more small-sized microbubbles, with the smallest size of 50–59 μm. It was found that there was a distribution of various microbubble sizes at a certain level of the water flow rate. However, the trend showed there was a more small-sized microbubble at higher water flow rates than at lower ones, as shown in Fig. 8.

4. Conclusion

The water flow rate used was in the range of 10–18m^3/h because previous experiments demonstrated that the air was not sucked in when the water flow rate was below 10 m^3/h. The experimental results showed that the air flow rate increased and the microbubble diameter decreased with an increasing water flow rate. When the airflow rate increased, the greater amount of sucked-in air would create more microbubbles. The results also showed that when the water flow rate was at 16 and 18 m^3/h, there was very little difference in terms of microbubble diameter. Considering size distribution, the smallest-sized microbubble obtained in the experiment was 50 μm.

Author statement

Kittipong Sakamatapan: Data curation. Mehrdad Mesgarpour: Conceptualization. Omid Mahian: Conceptualization. Ho Seon Ahn: Conceptualization, Formal analysis, Investigation, Writing - review & editing. Somchai Wongwises: Supervision, Formal analysis, Investigation, Writing – original draft.

Declaration of competing interest

We would like to say that we and our institution don't have any conflict of interest and don't have any financial or other relationship with other people or organizations that may inappropriately influence the author's work.

Acknowledgement

This work was supported by Incheon National University, Republic of Koreain 2019. The authors acknowledge the support provided by National Science and Technology Development Agency, Thailand. The authors would like to thank Mr. Jirayu Leelajiumjit and Mr. Sarunphat Kheawsuwan for their help in collecting some part of data upon which this paper is based.

References

[1] C.H. Lee, H. Choi, D.W. Jerng, D.E. Kim, S. Wongwises, H.S. Ahn, Experimental investigation of microbubble generation in the venturi nozzle, Int. J. Heat Mass Tran. 136 (2019) 1127–1138.

[2] J. Li, Y. Song, J. Yin, D. Wang, Investigation on the effect of geometrical parameters on the performance of a venturi type bubble generator, Nucl. Eng. Des. 325 (2017) 90–96.
[3] A. Gordiychuk, M. Svanera, S. Benini, P. Poesio, Size distribution and Sauter mean diameter of microbubbles for venturi type bubble generator, Exp. Therm. Fluid Sci. 70 (2016) 51–60.
[4] J. Yin, J. Li, H. Li, W. Liu, D. Wang, Experimental study on the bubble generation characteristics for an venturi type bubble generator, Int. J. Heat Mass Tran. 91 (2015) 218–224.
[5] X. Wang, Y. Shuai, H. Zhang, J. Sun, Y. Yang, Z. Huang, B. Jiang, Z. Liao, J. Wang, Y. Yang, Bubble breakup in a swirl-venturi microbubble generator, Chem. Eng. J. 403 (2021), 126397.
[6] A. Fujiwara, K. Okamoto, K. Hashigushi, J. Peixinho, S. Takagi, Y. Matsumoto, Bubble Breakup Phenomena in a Venturi Tube, 5th Joint ASME/JSME Fluids Engineering Conference, 2007, FEDSM2007, 37243.
[7] X. Vilaida, S. Kythavone, T. Iijima, Effect of throat size on performance of microbubble generator and waste water treatment, IOP Conf. Ser. Mater. Sci. Eng. 639 (2019), 012031.
[8] L.P. Afisna, W.E. Juwana, I. Indarto, D. Deendarlianto, F.M. Nugroho, Performance of porous-venturi microbubble generator for aeration process, Journal of Energy, Mechanical, Material, and Manufacturing Engineering 2 (2) (2017) 73–80.
[9] K.C. S Liew, A. Rasdi, W. Budhijanto, M.H.M. Yusoff, M.R. Bilad, N. Shamsuddin, N.A.H.M. Nordin, Z.A. Putra, Porous venturi-orifice microbubble generator for oxygen dissolution in water, Processes 8 (2020) 1266.
[10] B. Swart, Y. Zhao, M. Khaku, E. Che, R. Maltby, Y.M.J. Chew, J. Wenk, In situ characterisation of size distribution and rise velocity of microbubbles by high-speed photography, Chem. Eng. Sci. 225 (2020), 115836.
[11] N. Suwartha, D. Syamzida, C.R. Priadi, S.S. Moersidik, F. Ali, Effect of size variation on microbubble mass transfer coefficient in flotation and aeration processes, Heliyon 6 (2020), e03748.
[12] V. Bhadran, A. Goharzadeh, Monodispersed microbubble production using modified micro-venturi bubble generator, AIP Adv. 10 (2020), 095306.
[13] S. Shyam, B. Mehta, P.K. Mondal, S. Wongwises, Investigation into the thermo-hydrodynamics of ferrofluid flow under the influence of constant and alternating magnetic field by InfraRed Thermography, Int. J. Heat Mass Tran. 135 (2019) 1233–1247.
[14] P. Kaushik, P.K. Mondal, S. Chakraborty, Flow dynamics of a viscoelastic fluid squeezed and extruded between two parallel plates, J. Non-Newtonian Fluid Mech. 227 (2016) 56–64.
[15] S.R. Gorthi, H.S. Gaikwad, P.K. Mondal, G. Biswas, Surface tension driven filling in a soft microchannel: role of streaming potential, Ind. Eng. Chem. Res. 59 (9) (2019) 3839–3853.
[16] H.S. Gaikwad, D.N. Basu, P.K. Mondal, Non-linear drag induced irreversibility minimization in a viscous dissipative flow through a micro-porous channel, Energy 119 (2017) 588–600.